Chapter 3

Design and Proposal of a novel Biomass based Syngas production system integrated with Combined heat and Power Generation

In this chapter, a novel process model has been developed for biomass gasification integrated with combined heat and power generation for different types of biomasses which have been selected based on availability in abundant quantities from different regions of India. The influences of water to biomass ratio, reactor temperature and type of biomass on the amount of syngas produced, performance index etc. were studied. The model was developed using Aspen Plus, a chemical process simulator available commercially. The proposed model utilizes high thermal energy, carried by gasification products to operate a combined heat and power cycle consisting of two power cycles (steam and organic Rankine cycle) with provisions of heating air and water. The final product is syngas, a mixture of hydrogen and carbon monoxide, which has potential for many applications. The various output parameters such as total heat and work output along with efficiency for both cycles were tabulated. Afterwards, all of these data were used to select the appropriate biomass which would be suitable for the proposed model.

3.1. Proposed system layout

The schematic flow sheet of the model is shown in Fig.3.1. The system shows biomass and water entering the system through mixer (M) passing through pump (P-1). After the mixture enters into gasifier unit which is made up of two reactors: RYIELD and RGIBBS. Biomass (defined as a heterogeneous solid in Aspen Plus) does not have a defined molecular weight and is regarded as a non-conventional stream. For Aspen Plus to incorporate such a stream, the RYIELD reactor block is used to decompose it into its elementary, conventional components (C, H_2, O_2, N_2, Cl and S). The RGIBBS reactor block employs principle of Gibbs free energy minimization calculations in order to model chemical equilibrium at a specified temperature and pressure. A heat stream (Q-1) has been used to carry the heat of reaction from RYIELD to RGIBBS. This heat stream carries the external heat which has to be given to the RGIBBS to carry out the endothermic reactions. Another heat stream (Q-2) takes away net heat output from the RGIBBS reactor. This heat has to be supplied in order to maintain the isothermal conditions in the gasifier.

Now, the mixture of gasification reaction products released from the RGIBBS reactor were given to the heat exchanger (HX-1).The heat transfer in this heat exchanger was used to run the steam-rankine cycle as shown in Fig.1 by dotted lines. Another heat exchanger (WATERHTR) was used in the steam power cycle for water heating purpose using the waste heat of the cycle. The gasification products now go into the second heat exchanger (HX-2) where the heat extracted was used for operating ORC. There were also two additional heat exchangers used namely AIRHEATR and PREH. AIRHEATR was used for air heating whereas PREH was used as a pre-heater for the working fluid in the ORC.

Lastly, the mixture of gasification products was passed through a third heat exchanger (HX-3) which basically serves as a waste heat recovery unit. The temperature of the products was still much higher than the ambient temperature. So this heat exchanger was used to minimize the thermal pollution. The heat rejected in this heat exchanger was used for water heating purposes. After the third heat exchanger, the gasification products were passed to a separator (SEP) where they can be separated out into syngas and other products as required.

In the proposed system, gasification is carried out in the optimum temperature to produce maximum syngas. From domestic point of view, syngas as well as hydrogen production is extremely important besides former designs of gasification systems which were mainly based on economic and ecofriendly aspects (Damartzis et al., 2012; Kalina et al.,2010; Mertzis et al., 2014; Wang et al., 2014; Wang et al., 2016). Moreover, in the proposed model, there is an integration of biomass gasification with CHP which provides a wide variation of temperature in different processes, enabling power production by both organic Rankine and steam power cycles. This is because of the fact that the organic Rankine cycle is operated at low temperature whereas the steam power cycle is operated at relatively higher temperature. Hence, the special feature of the proposed system layout is CHP with maximum syngas production.

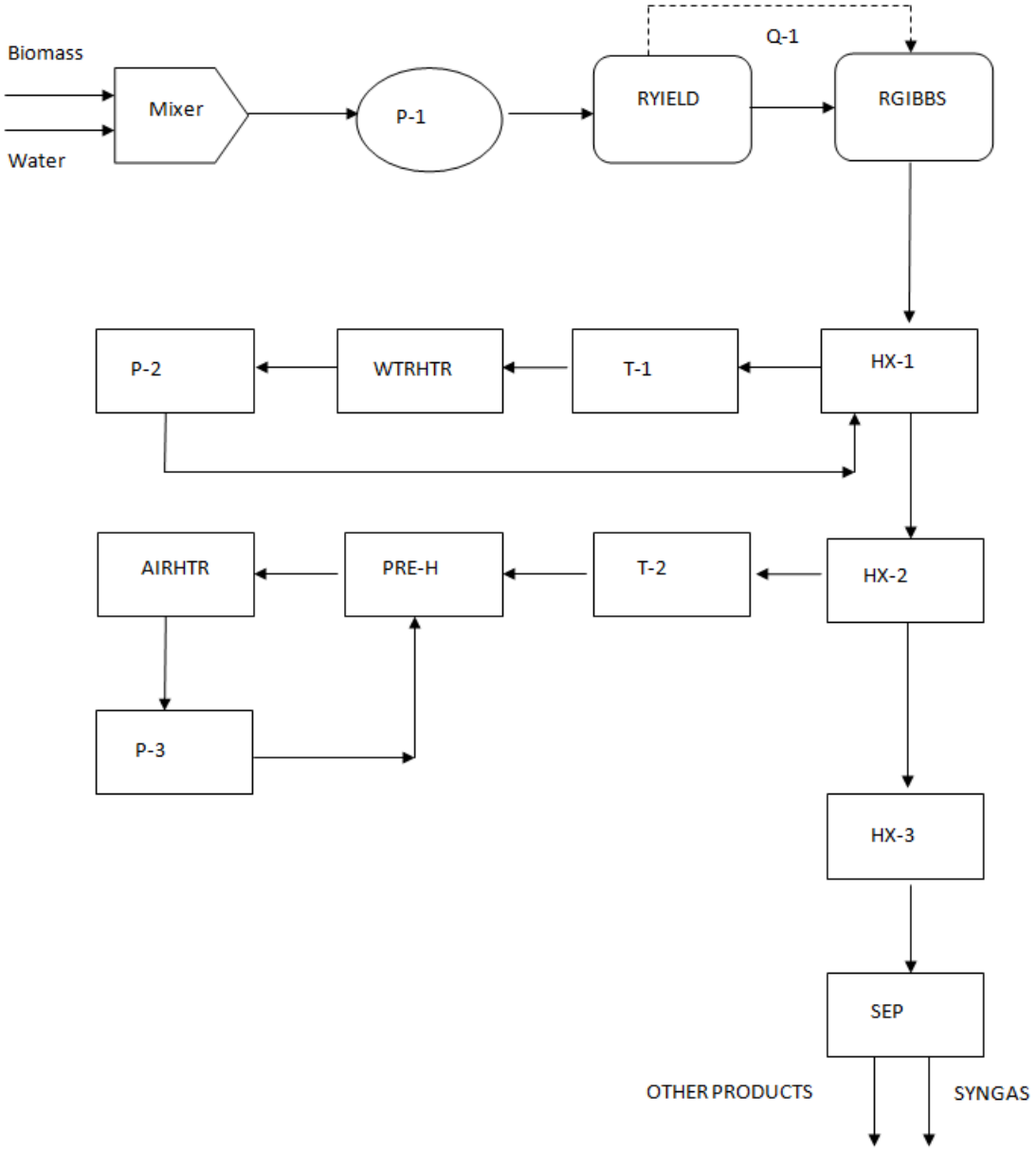

Fig. 3.1 Schematic flow sheet for the proposed model used in aspen simulation

3.2. Modelling and simulation

The following assumptions were considered in modeling the gasification process:

1. Gasifier is steady state system with uniform temperature and Pressure throughout.
2. Reactions of sulfur have not been taken into consideration.
3. Biomass devolatilization takes place instantaneously and volatile products mainly consist of H_2O, H_2, CO, CO_2, CH_4, C_2H_6, N_2, NO_2, NO, NH_3, O_2, and solid carbon($C_{(s)}$).
4. Pinch point temperature approach has been considered for heat exchanger modeling
5. Catalytic effects were not considered.
6. The working fluid in Rankine cycle is saturated liquid when it enters the pump.
7. The sink temperature for systems studied is 30°C and it was assumed that sufficient amounts of cooling water are available.
8. Turbine and pump have given isentropic efficiency
9. Heat transfer processes in all the heat exchangers are taken as isobaric.

The gasifying agent used is water. The components assumed to be present at equilibrium are $C_{(s)}$, CO, H_2, CO_2, H_2O, and CH_4. Based on the above assumptions, the global gasification reaction can be written as:

$$C_xH_yO_z + mH_2O \rightarrow aC_{(s)} + bCO + cCO_2 + dCH_4 + eH_2O + fH_2 \quad (3.1)$$

The concept of minimum Gibbs free energy at equilibrium can be applied in this non-stoichiometric modeling. The total Gibbs free energy (G^t) can be expressed as a function of temperature, pressure and the number of moles of i^{th} component (n_i) at equilibrium which is given by

$$G^t = f(T, P, a, b, c, d, e, f) \quad (3.2)$$

Considering minimum Gibbs free energy Eq. (3.2) can be written as:

$$dG^t = 0 \tag{3.3}$$

Now, using Eq. (3.3) molar flow rate of carbon, hydrogen and oxygen (x, y, z) can be determined from the following Eqs.:

$$x = a + b + c + d(\,for\ C - atom) \tag{3.4}$$

$$y + 2m \rightarrow 4d + 2e + 2f\,(\,for\ H - atom) \tag{3.5}$$

$$z + m \rightarrow b + 2c + e(\,for\ O - atom) \tag{3.6}$$

And the energy balance is given by (Ravikiran et al., 2012):

$$H_{\Pr od}(T) \rightarrow H_{react} + Q \tag{3.7}$$

Where,

$$H_{react} = H_{fuel} + m(\hat{H}^{O}_{f_{H_2O,298}} + \int_{298}^{T_{in}} C_{pH_2O}\,dT) \tag{3.8}$$

$$H_{prod}(T) = \sum_{prod} n_i \hat{H}^{O}_{fi,298} + \sum_{prod} n_i \int_{298}^{T} C_{p_i}\,dT \tag{3.9}$$

Enthalpy of fuel is calculated by,

$$H_{fuel} = m_{fuel} HHV - x\hat{H}^{O}_{f_{CO_2,298}} - \frac{y}{2}\hat{H}^{O}_{f_{H_2O,298}} \tag{3.10}$$

The fuel is specified as a non conventional component and higher heating value (HHV) of the fuel is calculated using the correlation proposed by Channiwala et al., 2002 as given in Eq. (3.11),

$$HHV = 341.9x + 1178.3y - 103.4z \tag{3.11}$$

Gasification reactions

Steam gasification of biomass can be represented by the chemical reactions Eq. (1.1)-(1.8) [Hirsch et al., 1982]. Eqs. (1.1) - (1.5) are regarded as the main gasification reactions. The gasification process may be split into steps: drying (at 100-200 °C), pyrolysis (at 200-500 °C), gasification and combustion.

Performance parameters

The steam rankine cycle and organic rankine cycle have been modeled based on the energy balance of each component (Sarkar et al., 2015). Isentropic efficiency has been used for pump and turbine, and fixed pinch point temperature approach has been used for evaporator and condenser.

Water to biomass ratio (WBR) and thermal efficiency (η) for the cycles were defined, respectively, as follows:

$$WBR = \frac{mass\ flow rate of\ water}{mass\ flow rate of\ Biomass} = \frac{\dot{m}_w}{\dot{m}_{fuel}} \tag{3.12}$$

$$\eta = \frac{Power\ \mathrm{Pr}oduced for individual cycle}{heat\ input for individual cycle} \tag{3.13}$$

A separate parameter was defined in order to judge the overall energy production of the model as *Performance Index*.

$$PI = \frac{Total\ Heat\ output + Total\ Power\ produced}{\dot{m}_{fuel} \mathrm{x}\ Calorific\ value} = \frac{Q_o + P}{\dot{m}_{fuel} \mathrm{x}\ CV} \tag{3.14}$$

Based on the above mathematical modeling, the simulation of proposed system has been carried out by ASPEN PLUS package. For given water-biomass rate, gasifier pressure (1 bar) and temperature, gasifier outlet condition has been evaluated first based on Gibbs free energy minimization and then the Rankine cycles have been simulated. The heat exchanger design has been carried out by minimum temperature approach. The temperature difference between hot stream inlet and cold stream outlet has been taken to be 30 K whereas the temperature difference between hot stream outlet and cold stream inlet saturation temperature has been taken to be 10 K. The isentropic efficiencies of turbine and pump have been taken as 0.9 and 0.85, respectively. The property method used is Peng-Robinson with Boston-Mathias alpha function (PR-BM). The PR-BM property method uses the Peng Robinson cubic equation of state with the Boston-Mathias alpha function for all thermodynamic properties. It gives reasonable results at all temperatures and pressures. Pump inlet temperature has been taken as 30 ^{0}C. Finally, the performance index has been determined.

The equilibrium results of the present numerical model have been validated with experimental results from the SCWG of glycerol (Byrd et al., 2008) as well as corn starch and sawdust (Antal et al., 2000). For the SCWG of glycerol (Table 3.1), the equilibrium yields of H_2 and CH_4 are in very good agreement with the experimental results (R^2 = 0.98 and R^2= 0.97, respectively). Although the equilibrium yields of CO_2 (R^2 = 0.83) and CO (R^2 = 0.75) fairly agree, it may be considered as acceptable. These deviations may be caused due to difference between the assumptions in ASPEN model and experimental conditions. For the SCWG of corn starch and sawdust (Table 3.2), most of the equilibrium yields of H_2, CH_4 and CO_2 show good agreements and yield of CO shows fair agreement with experimental

results according to the values of R^2.

In this chapter, performances of different biomass materials have been compared to select the suitable one. Hence, the biomass materials have been selected based on availability in India. The ultimate analysis of selected biomass materials are shown in Table 2.1.

Table 3.1 Thermodynamic equilibrium yields vs experimental gas yields (mol/ molglycerol) for Supercritical water gasification of glycerol, Byrd et al., 2008 at various temperatures and feed concentrations and constant pressure of 24.1 MPa

FEED (wt.%)	T[^{O}C]	PRODUCT GAS YIELD(mol/mol$_{glycerol}$)							
		Present Study				Experimental results			
		H_2	CH_4	CO	CO_2	H_2	CH_4	CO	CO_2
5	800	6.72	0.09	0.18	2.76	6.54	0.32	0.1	2.36
15	800	4.63	0.49	0.36	2.11	4.13	0.72	0.04	2.21
20	800	3.77	0.71	0.36	1.91	3.94	0.81	0.17	2.42
30	800	2.67	0.99	0.38	1.62	2.87	0.92	0.21	2.07
35	800	2.28	1.09	0.38	1.52	2.6	0.95	0.24	1.93
40	800	1.97	1.16	0.37	1.44	2.18	0.94	0.24	1.79
50	700	6.05	0.18	0.09	2.66	5.12	0.49	0.02	2.34
5	750	6.53	0.09	0.18	2.76	5.81	0.29	0.01	2.50
5	800	6.72	0.09	0.18	2.76	6.54	0.29	0.09	2.34
	COV	0.432	0.837	0.419	0.263	0.379	0.454	0.746	0.107
	R^2					0.98	0.97	0.75	0.83

Table 3.2 Thermodynamic equilibrium vs experimental gas composition (dry mole fraction) for Supercritical water gasification of glycerol of corn starch (CS) & sawdust (SD) mixtures (Antal et al., 2000]) at various temperatures and 28 MPa

FEED (wt.%)	T[^{O}C]	PRODUCT GAS YIELD(dry mole fraction)							
		Present Study				Experimental Results			
		H_2	CH_4	CO	CO_2	H_2	CH_4	CO	CO_2
10.4	650	0.45	0.15	0.01	0.37	0.47	0.15	0.02	0.37
13.7	715	0.48	0.12	0.02	0.36	0.55	0.06	0.02	0.34
10.72SD+4.01CS	685	0.41	0.18	0.03	0.38	0.43	0.17	0.03	0.38
	R^2					0.92	0.88	0.74	0.92

3.3 Results and discussion

The model has been investigated for five water to biomass ratios (0.2, 0.4, 0.6, 0.8 and 1.0), four total mixture mass flow rates (50 kg/ h, 60 kg/h, 70 kg/h and 80 kg/h) and ten different biomass materials (see Table 2.1). First step of the simulation is to determine optimum gasification temperature yielding maximum syngas production for all five water to biomass ratios and all biomass materials. For this purpose a graphical plot of syngas and H_2 production with respect to gasification temperature has been drawn for each biomass material under different conditions. Fig. 3.2 depicts the variation of yield of syngas with gasification temperature (K) for Leather Waste (LW). As observed, there is some optimum temperature, which yields maximum syngas production and this is true for all biomass. The obtained optimum gasification temperatures for all cases have been used to simulate the rest of the model and calculate the required performance index. Results for three cases: case 1. Keeping total mass flow rate constant with variation in WBR (Figs. 3.2-3.6), case 2. Varying total mass flow rate (TMF) but keeping WBR = 0.4 (constant) (Figs. 3.7-3.11) and case 3. Comparison of all biomass with TMF =50 kg/h (constant) and varying WBR (Figs. 3.12-3.16) are presented.

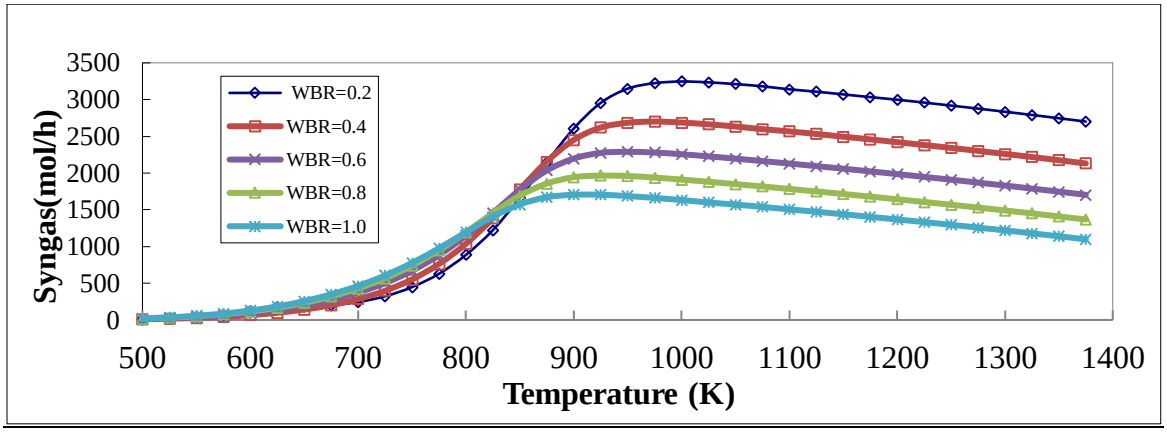

Fig. 3.2. Plot of syngas (mol/h) vs. gasification temperature (K) for leather waste with constant total mass flow rate but with varying water to biomass ratio

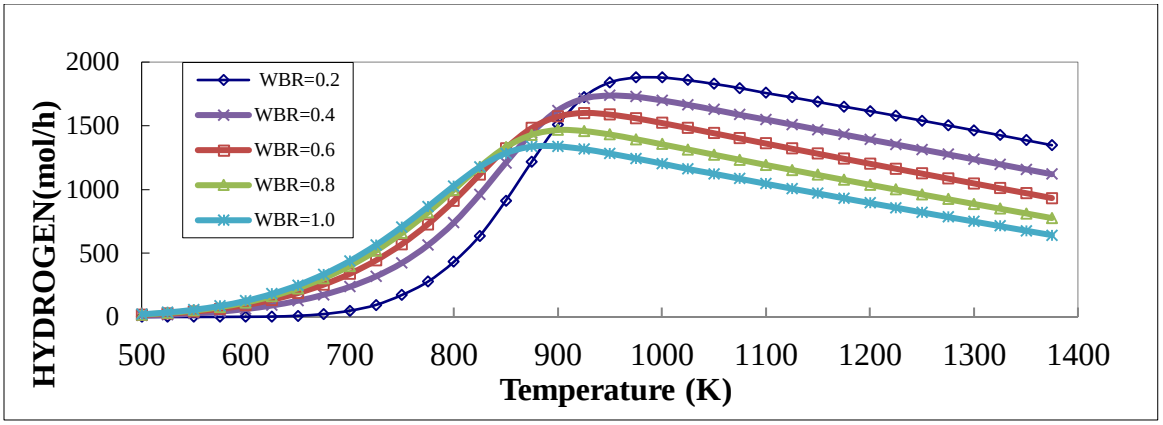

Fig. 3.3 Plot of hydrogen gas (mol/h) vs. gasification temperature (K) for with constant total mass flow rate but with varying water to biomass ratio

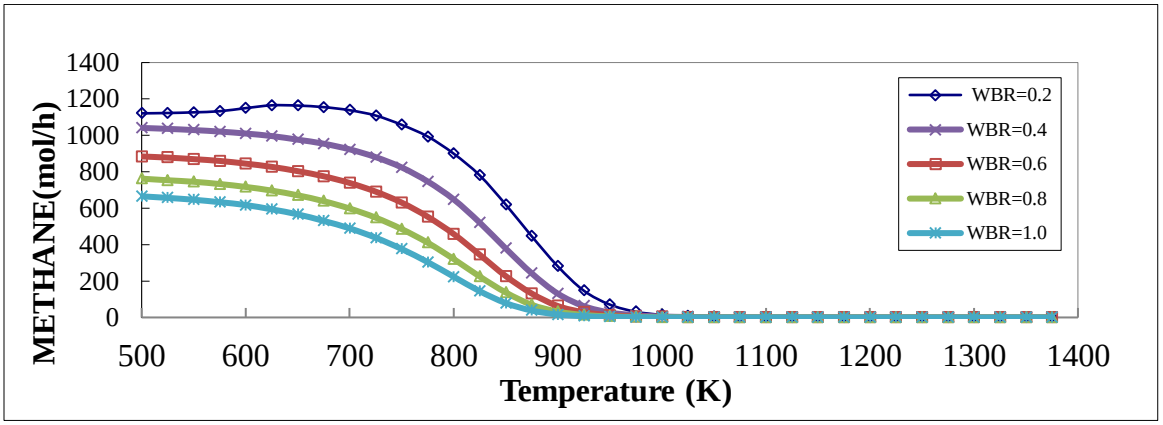

Fig. 3.4 Plot of methane gas (mol/h) vs. gasification temperature (K) for with constant total mass flow rate but with varying water to biomass ratio

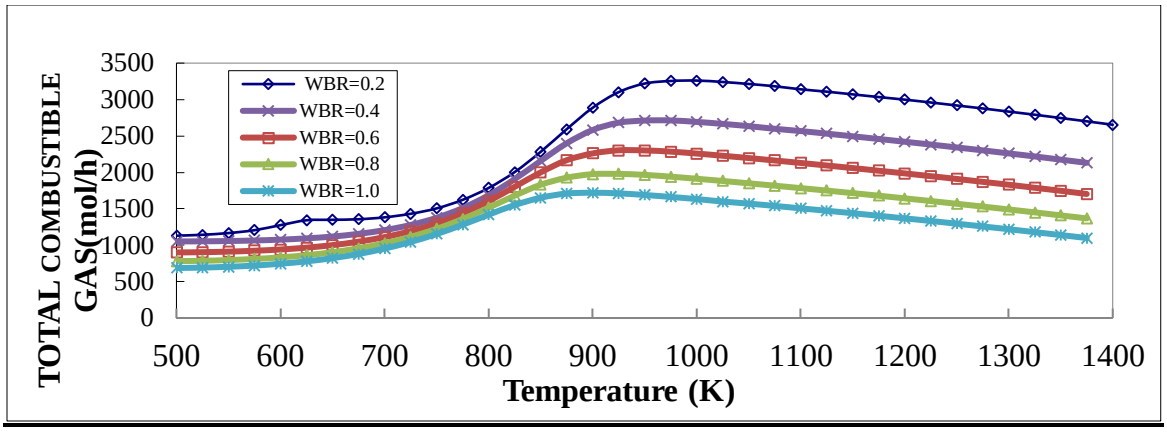

Fig. 3.5 Plot of Total combustible gases (mol/h) vs. gasification temperature (K) for with constant total mass flow rate but with varying water to biomass ratio

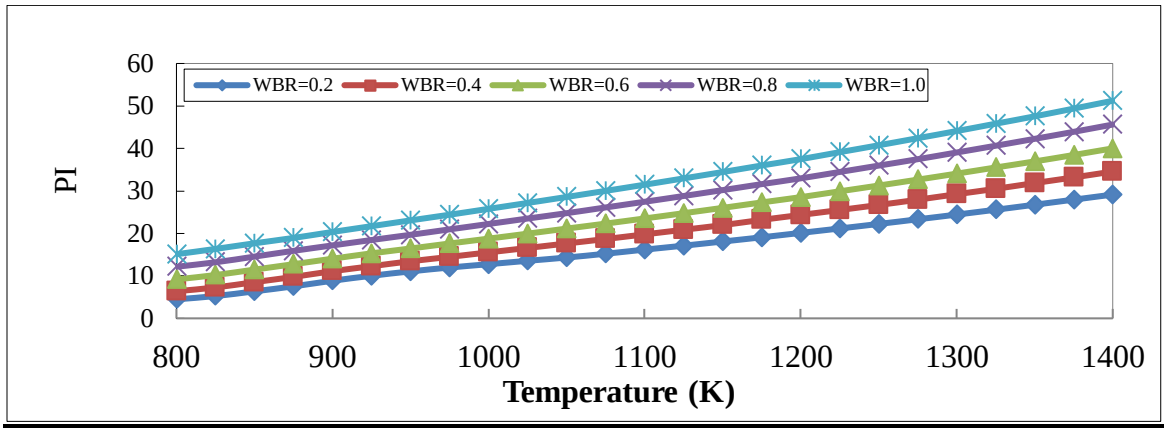

Fig. 3.6 Plot of Performance index vs. gasification temperature (K) for with constant total mass flow rate but with varying water to biomass ratio

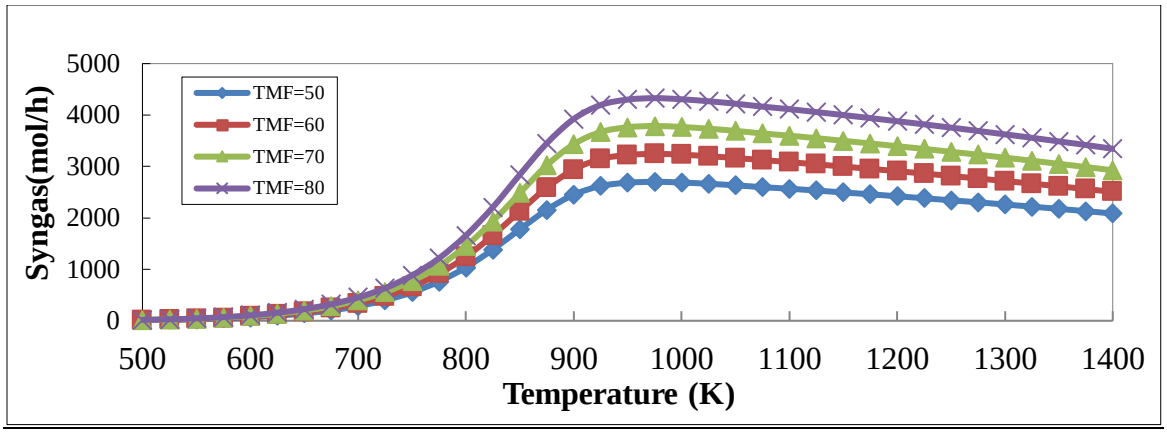

Fig. 3.7 Plot of syngas (mol/h) vs. gasification temperature (K) for Leather waste with constant water to biomass ratio (=0.4) but with varying total mass flow rate

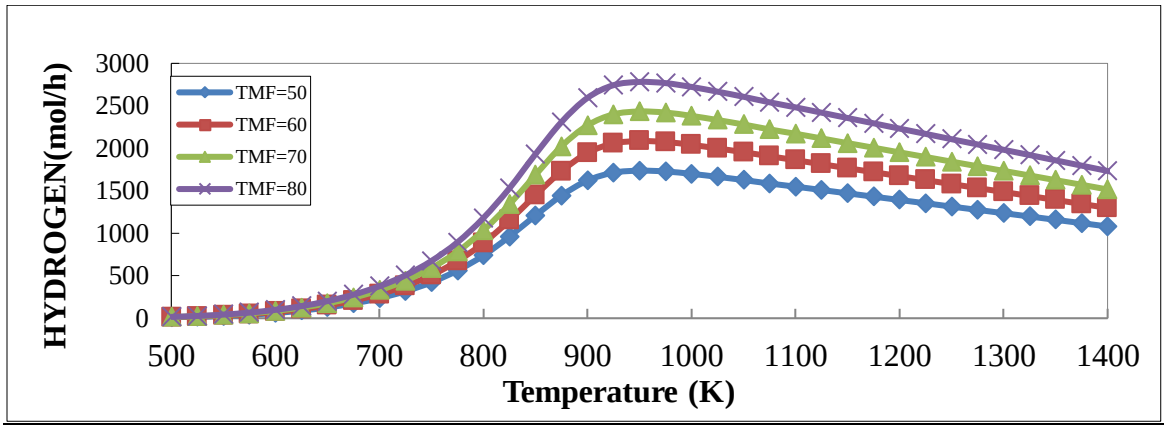

Fig. 3.8 Plot of hydrogen gas (mol/h) vs. gasification temperature (K) for Leather waste with constant water to biomass ratio (=0.4) but with varying total mass flow rate

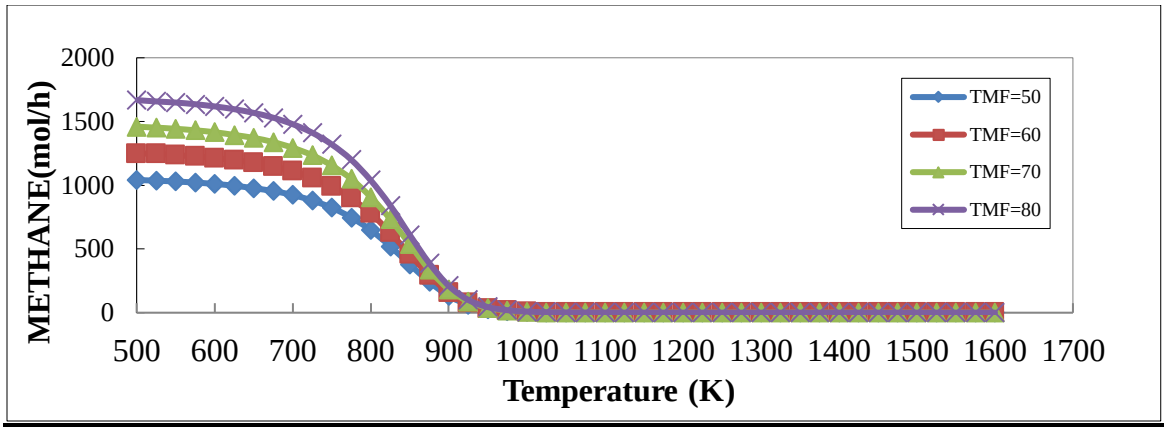

Fig. 3.9 Plot of methane gas (mol/h) vs. gasification temperature (K) for Leather waste with constant water to biomass ratio (=0.4) but with varying total mass flow rate

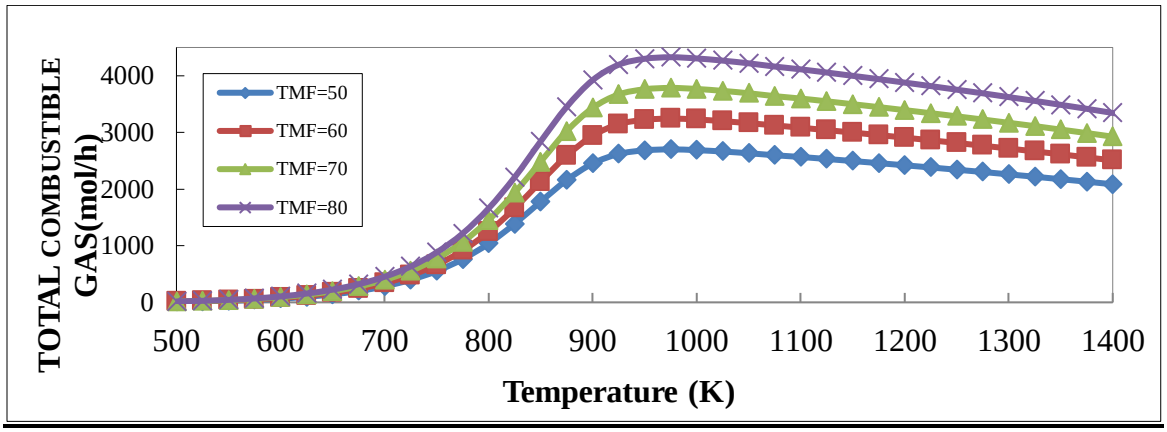

Fig. 3.10 Plot of Total combustible gases (mol/h) vs. gasification temperature (K) for Leather waste with constant water to biomass ratio (=0.4) but with varying total mass flow rate

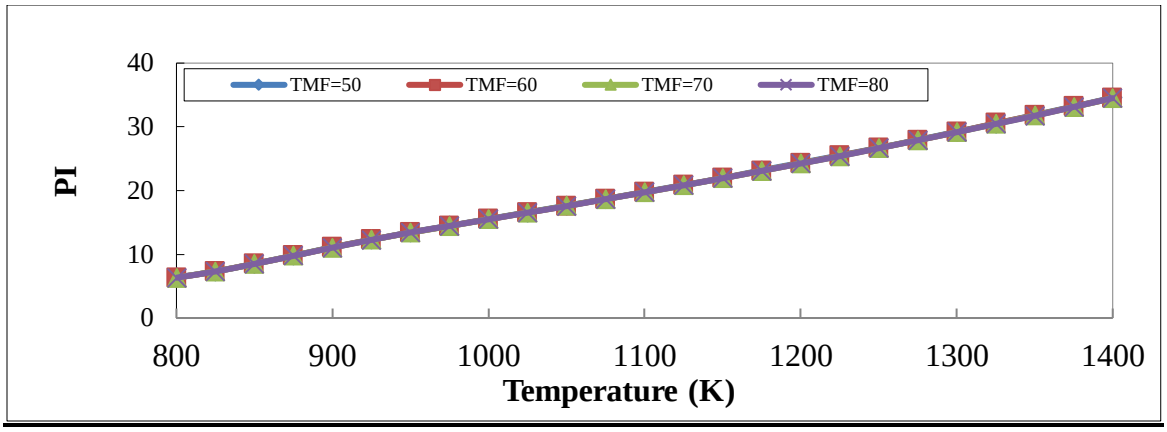

Fig. 3.11 Plot of Performance index vs. gasification temperature (K) for Leather waste with constant water to biomass ratio (=0.4) but with varying total mass flow rate

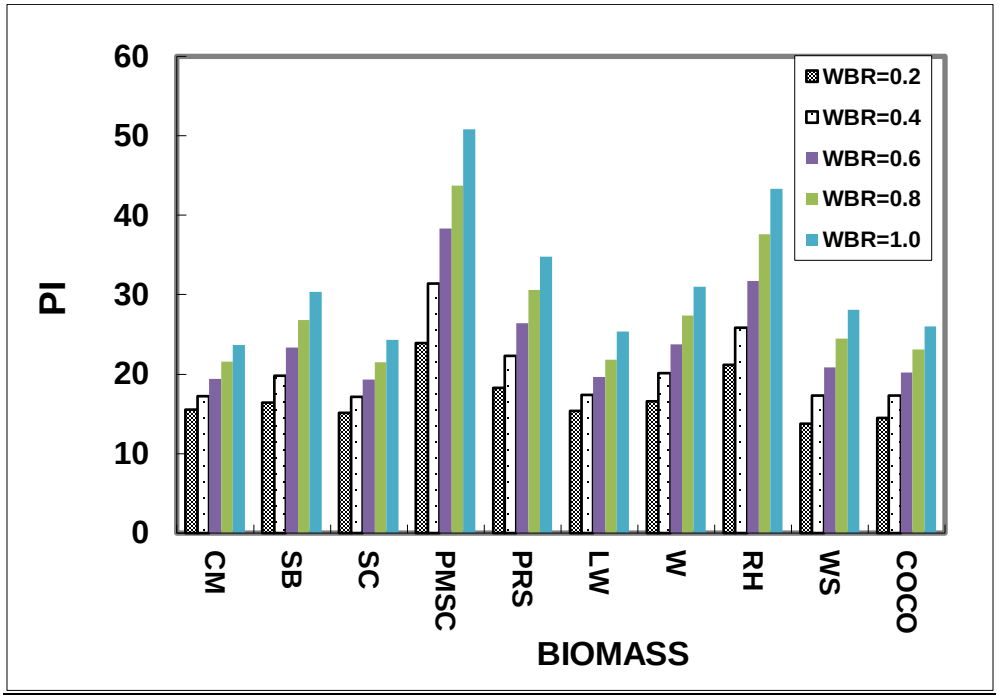

Fig. 3.12 Performance Index of all biomasses with total mass flow rate constant and varying water to biomass ratio

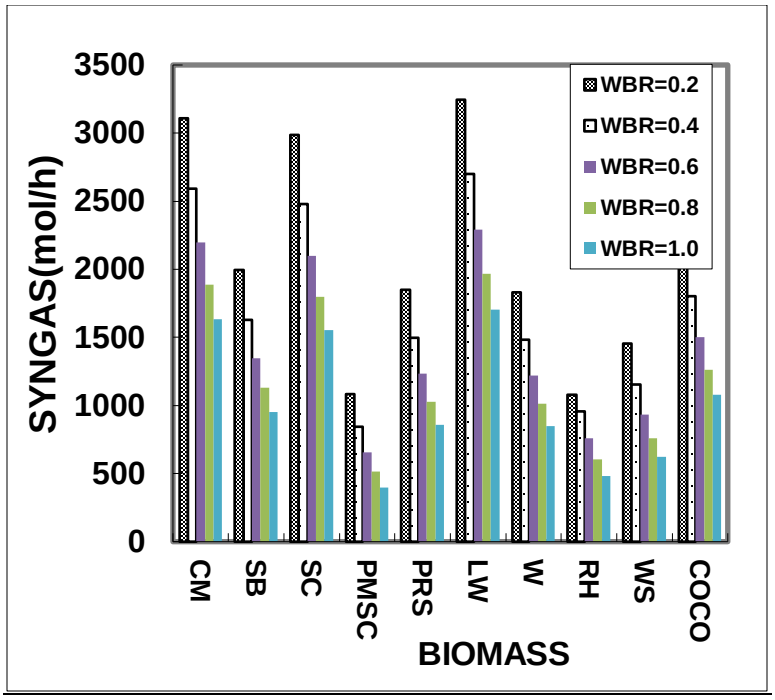

Fig. 3.13 Number of moles of syngas produced for all biomasses with constant total mass flow rate and varying water to biomass ratio

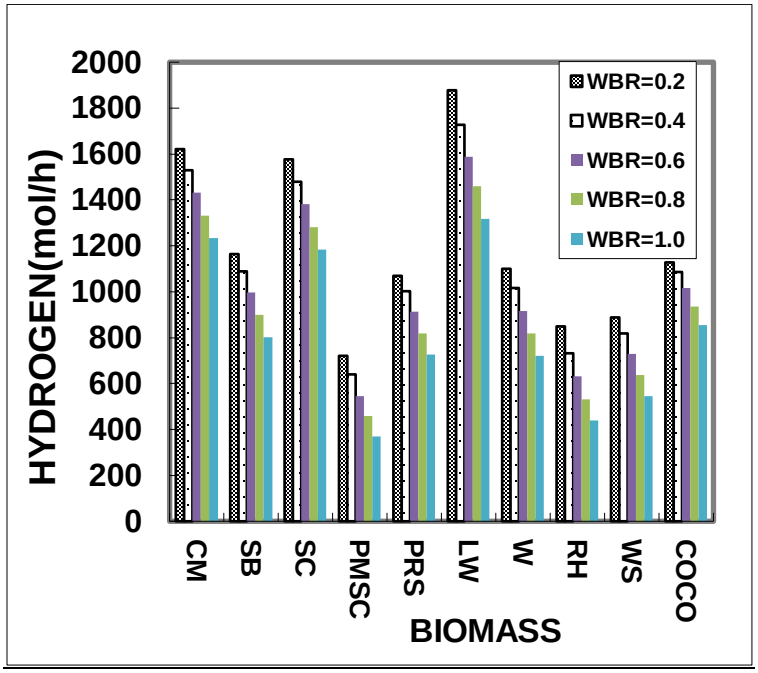

Fig. 3.14 Number of moles of hydrogen produced for all biomasses with constant total mass flow rate and varying water to biomass ratio

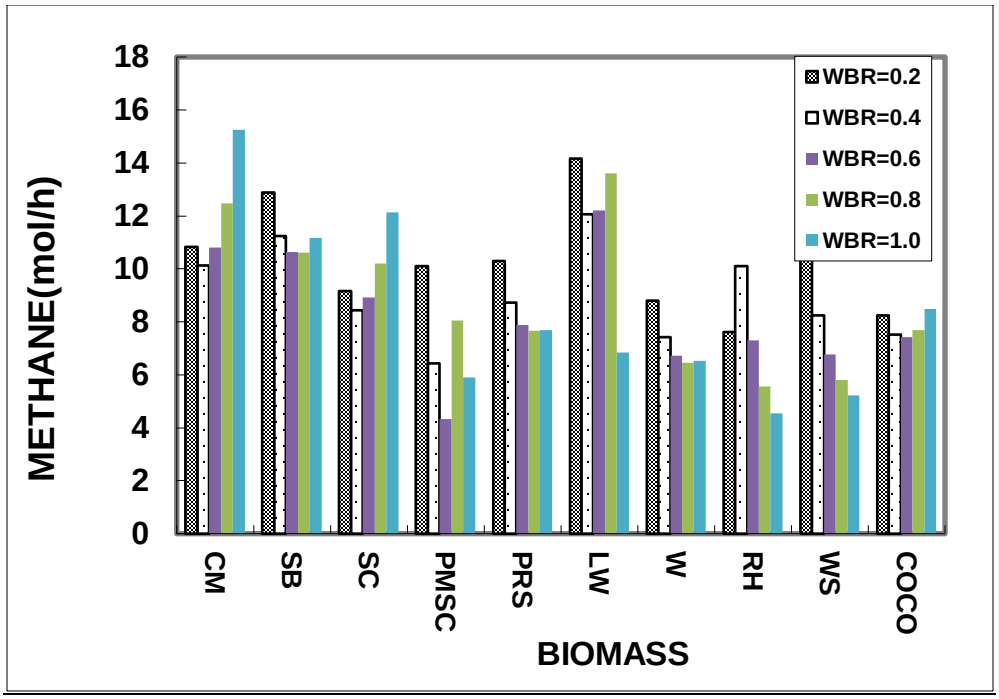

Fig. 3.15 Methane gas produced for all biomasses with constant total mass flow rate and varying water to biomass ratio

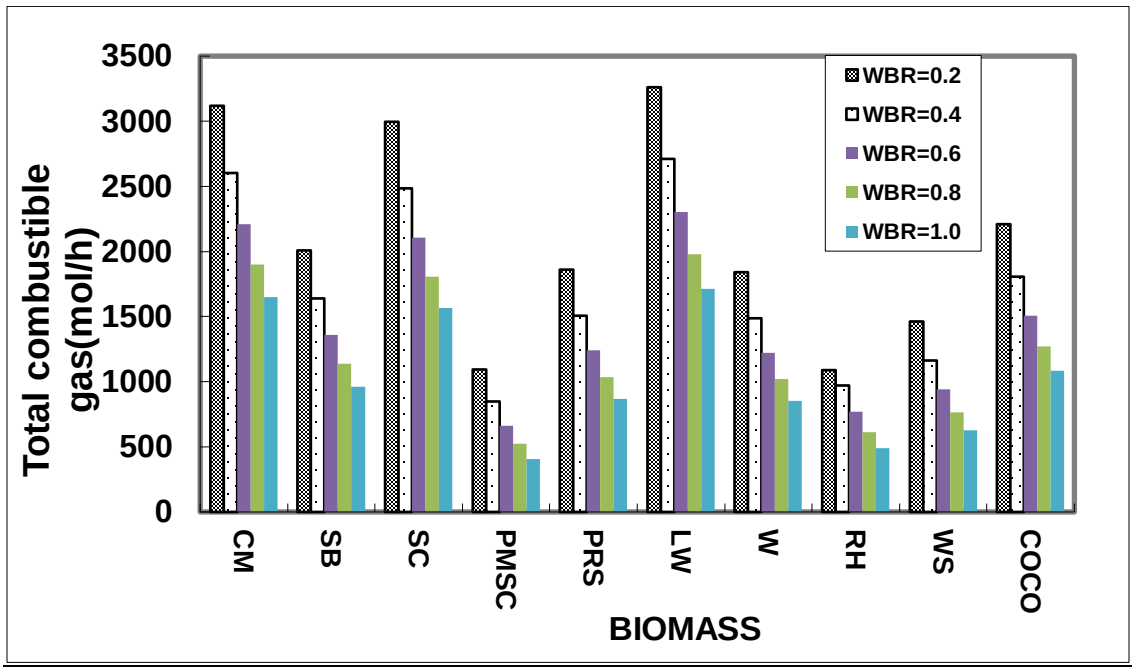

Fig. 3.16 Total combustible gases produced for all biomasses with constant total mass flow rate and varying water to biomass ratio

For sensitivity analysis, four inlet parameters such as water-biomass ratio, total mass flow rate, temperature of gasification and ten different biomass materials were considered with five output parameters such as syngas, methane, PI, hydrogen and total combustible gas. Air was supplied in gasifier which was required to maintain the process slightly exothermic. However, air flow rate is not considered as an inlet parameter. The observations for this sensitivity analysis are discussed below:

A) **Effects of temperature and WBR at a constant total mass flow rate (TMF)**

The moles of syngas produced increases as the gasification temperature increases upto a maximum value and then decreases as the temperature further increases (Fig. 3.2). This optimum temperature for obtaining maximum amount of syngas, which is different for different biomass, is higher for lower WBR values. According to Le Chatelier's principle, higher temperatures favor the reactant side in exothermic reactions whereas in endothermic reactions it favors the product side. Hence, the yield of syngas increases with increase in gasification temperature upto the optimum value as observed. However, reverse water gas shift dominates at higher temperatures and it leads to decrease in concentration of H_2 (Fig. 3.3). The CO content is affected by Boudard reaction (Eq. (1.3)) and it is an exothermic reaction. Hence, the content of CO decreases when temperature increases. Further, syngas production is found to be increased as WBR decreases, for higher gasification temperatures than optimum value. However, at lower gasification temperatures than optimum value, as WBR increases, moles of syngas produced also increase. This may be possible due to water gas reaction favoring forward reaction at high temperature to give more H_2 and CO whereas at low temperature the reaction runs backwards, so more water mass flow rate produces more

syngas (H_2 and CO). Higher WBR means less biomass which implies that there is not enough biomass to react with water and so, wateregas reactions, steam reforming and mainly wateregas shift reaction are left incomplete. Therefore, with increase in WBR, H_2 and CO concentrations decrease in the products. Steam-reforming (Eq. (1.8)) and methanation (Eq. (1.6)) reactions can be considered for methane gas production, out of which the former reaction is endothermic and latter one is exothermic in nature. Therefore, when the temperature increases, methanation reaction shifts towards reactant sides decreasing methane production. But at high temperature, steam reforming reaction dominates over methanation reaction and hence decrease in the yield of methane occurs mainly due to this. Therefore, the yield of methane is found to be inversely proportional with gasification temperature (Fig. 3.4). It is found to be maximum at lower temperatures and negligible at higher temperatures. The methane gas follows same behavior with WBR as it does with gasification temperature. When more water is added to the system, steam reforming reaction favors the products side and hence, the concentration of methane decreases. There is a sudden increase in methane yield between temperature 600 K-750 K at WBR = 0.2. This may be due to the fact that water gas reaction dominates in this temperature range, so more CO and H_2 are produced which shifts the steam reforming reaction to the reactant side producing more methane in combination with methanation reaction as temperature increases in this temperature range. The total combustible gases (consisting of syngas and methane gas) obtained is shown in Fig. 3.5, it follows the same trend as the syngas. It can be easily observed that at lower temperature, the moles of syngas produced are found close to zero whereas the moles of total combustible gases are observed to be in significant numbers. This is due to the fact that at lower temperature, though syngas production is negligible, methane production is significant

which would render the reported number of moles of total combustible gases. The Performance Index (PI) increases with WBR and the magnitude of PI is higher at a higher temperature. The variation of PI with gasification temperature for LW is shown in Fig. 3.6. The thermal efficiency of the hybrid system is found to be in the range of 0.36-0.39 for steam Rankine cycle and 0.28-0.29 for organic Rankine cycle for all the biomass materials under consideration. The thermal efficiency is lower at higher values of water to biomass ratio and higher at lower water to biomass ratio. The range of temperatures has been taken as 800-1400 K.

B) Effects of temperature and total mass flow rate (TMF) at a fixed WBR (0.4)

From the results of the previous case, it is clear that for lower WBR values, the syngas and hydrogen productions are more than at higher WBR values. However, WBR = 0.4 has been taken for analysis of this case instead of WBR = 0.2 because water mass flow rate for the latter case is very less and taking WBR = 0.2 results unpredicted outcomes as shown in the previous section. The syngas yield shows similar trend with the gasification temperature, as observed for the previous case. More syngas is produced at higher TMF values as shown in Fig. 3.7. The gasification temperature, for which, maximum yield of syngas is obtained, has been taken as optimum gasification temperature and it found to be independent of TMF values. In other words, TMF has no effect on the optimum gasification temperature. The hydrogen production is found to have a direct relationship with gasification temperature as well as with TMF (Fig. 3.8). The higher value of the TMF implies presence of higher amount of biomass in the system which reacts to produce more products than at lower TMF values. The methane gas yield decreases with increase in temperature which is the observation as reported in the previous section. The

variation of methane gas is shown in Fig. 3.9. The methane shows the same direct proportionality behavior with TMF as well. The total combustible gases (including syngas and methane) yield is shown to follow the same behavior as the syngas (Fig. 3.10). The Performance Index (as it is a ratio) does not depend on TMF, as shown in Fig. 3.11.

C) Performance comparison of biomass materials at optimum gasification temperature

The Performance Index shows an overall increasing trend concerning its dependency on the WBR (Fig. 3.12) when comparing all the biomass materials. The maximum PI has been observed for PMSC (50.8%). The production of syngas increases as WBR decreases for a fixed optimum temperature for each biomass material. The maximum syngas has been found for LW (3246 mol/h), as shown in Fig. 3.13. The hydrogen production has been found to have an inverse relationship with WBR. The maximum hydrogen yield is 1878 mol/h for LW, as shown in Fig. 3.14. The methane gas production has been found to have no fixed trend with WBR (Fig. 3.15). But it may be due to the reason that the methane yield is very low at the particular optimum gasification temperature for each WBR compared to yield of other gases. The moles of total combustible gases (including syngas and methane) produced have been shown to follow the same trend as the syngas, as shown in Fig. 3.16. The yield of total combustible gases is much higher than the yield of CO_2, which means that it can be used for domestic purposes easily. The yield of total combustible gases has been found to be 3260 mol/h for LW, which is the highest among all other biomass samples. Cow manure, Leather waste and coconut shell have higher efficiency when compared to other biomass materials.